VIRUS EVOLUTION

Virus Evolution, 2025, **11(1)**, veaf022

DOI: https://doi.org/10.1093/ve/veaf022
Advance Access Publication 19 April 2025
Research Article

Virome of *Hyalomma* and *Rhipicephalus* ticks from desert of Northwestern China

Ning Wang[1,‡], Shan Lu[1,‡], Run-Ze Ye[2,3,‡], Cheng Li[1], Jiang-He Huang[4], Gang Ye[4], Yu-Yu Li[5], Shi-Jing Shen[1], Xiao-Yu Shi[3], Dai-Yun Zhu[3], Wenqiang Shi[3], Lin Zhao[1], Na Jia[3], Jia-Fu Jiang[3], Xiao-Ming Cui[3], Yi Sun[3,*], Wu-Chun Cao[1,3,5,*]

[1]Institute of EcoHealth, School of Public Health, Cheeloo College of Medicine, Shandong University, Jinan, Shandong 250012, P. R. China
[2]Department of Emergency Medicine, Qilu Hospital of Shandong University, Jinan, Shandong 250012, P. R. China
[3]State Key Laboratory of Pathogen and Biosecurity, Academy of Military Medical Sciences, Beijing 100071, P. R. China
[4]Karamay Center for Disease Control and Prevention, Karamay, Xinjiang 834000, P. R. China
[5]Research Unit of Discovery and Tracing of Natural Focus Diseases, Chinese Academy of Medical Sciences, Beijing 100071, P. R. China

[‡]These authors contributed equally to this article.
* Corresponding authors. Wu-Chun Cao, Institute of EcoHealth, School of Public Health, Cheeloo College of Medicine, Shandong University, Jinan, Shandong 250012, P. R. China. E-mail: caowuchun@126.com; Yi Sun, State Key Laboratory of Pathogen and Biosecurity, Academy of Military Medical Sciences, Beijing 100071, P. R. China. E-mail: 378176938@qq.com.

Abstract

Ticks are important vectors for pathogen transmission, yet studies on the diversity and distribution of viruses carried by ticks in desert regions remain limited. This study investigated the tick virome in desert areas of Xinjiang, China, and identified two tick species, *Hyalomma asiaticum* and *Rhipicephalus turanicus*. A total of 30 meta-transcriptome sequencing libraries were constructed from ticks pooled by location, tick species, sex, and host. The proportion of viral reads ranged from 0.004% to 0.165%, and significant differences in viral alpha- and beta-diversity were observed between the two tick species. A total of 125 complete or nearly complete viral genomes were classified into 5 families of positive-sense single-stranded RNA viruses, 6 families of negative-sense single-stranded RNA viruses, and 2 families of double-stranded RNA viruses. Twenty-eight viral species were identified, including 20 known viruses and 8 novel viruses from the genera *Orthonairovirus, Quaranjavirus*, and *Mitovirus*, and families *Peribunyaviridae* and *Narnaviridae*. Notably, the discovery of Desert orthonairovirus, Desert quaranjavirus, and Desert peribunya-like virus revealed a potential new role for desert ticks as viral vectors. Among the other 25 viruses, 12 were specific to *H. asiaticum*, and 9 were specific to *R. turanicus*. This study highlights the diversity of tick-borne viruses in Xinjiang's desert regions, their distribution across different tick species, and underscores the importance of these tick species in pathogen transmission. These findings provide scientific evidence for further research into viral circulation in desert ecosystems and the potential public health threats posed by tick-borne pathogens.

Keywords: emerging tick-borne virus; tick virome; desert; *Hyalomma asiaticum*; *Rhipicephalus turanicus*

Introduction

Tick-borne diseases (TBDs) represent a significant global public health challenge, but they remain neglected (Zhou et al. 2023). Ticks exhibit remarkable environmental adaptability, enabling them to survive in a range of ecosystems, including extreme desert and semi-desert environments (Jia et al. 2020). In recent years, emerging tick-borne viral infections have been increasing (Wang et al. 2019, Liu et al. 2020, Zhang et al. 2024, 2025), but the study of TBDs in desert regions remains insufficient, highlighting the urgent need for further research in these environments.

Desertification has become a major global environmental concern, affecting ~36 million square kilometers, or one-quarter of the world's total land area (Pal et al. 2023). China is one of the countries with the most severe desertification, mainly concentrated in the northwestern regions such as Xinjiang and Inner Mongolia (Li et al. 2021). As ecological restoration and desertification control projects progress (Bryan et al. 2018), some desert areas are gradually being transformed into oases. Although this transformation enhances regional biodiversity, it also increases the likelihood of contact between ticks and their hosts. Furthermore, increased human activities such as grazing and ecological restoration in desert areas, coupled with a growing number of tourists exploring diverse desert landscapes, provide more opportunities for tick-human contact, thereby amplifying the risk of tick-borne pathogen transmission.

Here, we collected ticks from desert ecosystems in Xinjiang, China, and conducted the meta-transcriptome sequencing to

investigate the diversity and characteristics of the viruses of desert ticks. The aim of this study was to characterize the virome of desert ticks, identify novel viruses, explore the relationships between desert ticks and viruses, and assess their potential public health threats.

Methods

Sample collection and data management

Tick samples were collected in Xinjiang, China, in 2023, with sampling sites selected based on the ecological environment. Free-living ticks were collected by the human attraction method, which relies on ground vibrations generated by footsteps, whereas parasitic ticks were gathered from livestock. The latitude and longitude of each site were recorded. The species, sex, and developmental stage of each tick were identified by an entomologist. Live ticks were transported to the laboratory and thoroughly sterilized (two successive washes of 75% ethanol for 30 s) and then transferred to a −80°C storage freezer. The geographical distribution of ticks was plotted using ArcGIS 10.2 software.

RNA extraction, library preparation, and sequencing

Adult ticks were divided into pools based on tick species, sex, sampling site, and host. Extraction of total DNA and RNA from pools of ticks was performed using the AllPrep DNA/RNA mini kit (Qiagen) with modifications. Briefly, ticks were homogenized in Buffer RLT Plus (lysis buffer) under liquid nitrogen. The lysate was pipetted directly into a QIAshredder spin column placed in a 2 ml collection tube and centrifuged for 2 min at maximum speed. The homogenized lysate was transferred to an AllPrep DNA spin column and centrifuged for 30 s at 8000*g*. The AllPrep DNA spin column was used for later DNA purification, and the flow through was used for RNA purification following the manufacturer's instructions. The purified RNA was quantified using Qubit 4.0 fluorometer, and RNA quality was assessed using an Agilent Bioanalyzer 2200 (Agilent). All RNA extractions in this study had an amount ≥1 ng and an RNA integrity number >5.8. Ribosomal RNA was removed using RiBo-Zero Gold rRNA removal reagents (Human/Mouse/Rat) (Illumina). The sequencing library was then prepared following the Illumina standard protocol. Paired-end (2 × 150 bp) sequencing (RNA-seq) was conducted on an Illumina NovaSeq 6000 platform.

Viral contig assembly and annotation

Raw paired-end sequence reads were first quality controlled using AfterQC (v2.3.3) (Chen et al. 2017), and host-related reads were removed by mapping against the tick genomes (GCA_013339685.2 and PRJNA1131278) downloaded from the NCBI using Bowtie2 (v2.3.5.1) (Langmead and Salzberg 2012). Clean reads were *de novo* assembled into contigs using Trinity (v2.13.2) (Grabherr et al. 2011). The assembled contigs were compared to the NCBI non-redundant protein database using Diamond BLASTx (v2.0.13) (Buchfink et al. 2021) and the NCBI nucleotide sequence database using BLASTn (v2.12.0+) (Camacho et al. 2009) to identify virus-related contigs, with an *E*-value threshold of $<1 \times 10^{-5}$ to achieve high sensitivity while reducing false positives. Contigs associated with tick genomes, identified through BLAST analysis, were excluded from downstream analysis to eliminate any potential endogenous viral elements.

The coding sequence (CDS) of virus sequences was annotated using Geneious Prime v2024.0.7 (https://www.geneious.com). The RNA-dependent RNA polymerase (RdRp) domain was identified by comparison with the Conserved Domain Database (https://www.ncbi.nlm.nih.gov/Structure/cdd/wrpsb.cgi). Species classification of the virus sequences was performed according to the International Committee on Taxonomy of Viruses (ICTV) reports (https://talk.ictvonline.org/ictv-reports/ictv_online_report/). For viruses lacking clear species classification standards within a genus, the RdRp protein was aligned with a threshold of 90% amino acid similarity. If the similarity of conserved regions exceeded 90% with known virus sequences, the virus was classified as the same species; otherwise, it was considered a novel viral species (Shi et al. 2016). The naming of novel viruses was combining 'Desert' with the genus or family of the virus, excluding the 'viridae' suffix. Novel virus sequences were confirmed by checking read coverage and continuity using Bowtie2.

Quantification of tick virome abundance and diversity

We quantified the abundance of each viral family in each library as the number of viral reads per million non-host reads by mapping clean reads of each library to the NCBI nucleotide sequence database (nt, version 2024/05/30) using Kraken2 (v2.1.3) (Lu et al. 2022). Non-viral reads, such as bacterial and eukaryotic-related reads, were excluded from downstream analysis. If the viral reads were not assigned to any defined family and assigned to unclassified Riboviria [txid 2585030] or unclassified viruses [txid12429], they were designated as 'unclassified viruses'. Additionally, as the reference database included tick genome sequences, this step also helped eliminate potential endogenous viral elements. Alpha diversity of viruses in each sample was evaluated using Kraken tools. For beta diversity (between-library dissimilarity) analysis, principal coordinates analysis (PCoA) was performed and visualized with the vegan package in R software (Oksanen et al. 2024). A two-sided Student's *t*-test was employed to investigate differences in viral diversity among tick species. *P*-values <.05 were considered statistically significant.

Phylogenetic analysis

Phylogenetic analysis was conducted based on the CDS containing the conserved region of RdRp in the viral genome. We initially performed a BLAST analysis (https://blast.ncbi.nlm.nih.gov/Blast.cgi) on the assembled sequences, followed by the inclusion of complete or nearly complete sequences with the highest sequence similarity. Additionally, sequences from the same family or genus were included. Based on the phylogenetic trees, redundant sequences with distant genetic relationships were removed. The assembled sequences were then aligned with related sequences downloaded from GenBank by using the E-INS-i/L-INS-i algorithm implemented in MAFFT (v7.490) (Rozewicki et al. 2019). Ambiguous regions in the alignment were trimmed using TrimAl (v1.4) (Capella-Gutiérrez et al. 2009). The IQ-TREE (v2.2.2.3) algorithm (Nguyen et al. 2015) was used to determine the best-fit amino acid or nucleotide substitution model based on each multiple sequence alignment. A maximum likelihood phylogenetic tree was constructed with 1000 bootstrap replicates using IQ-TREE and was visualized using the ggtree (Yu et al. 2018), phangorn (Schliep 2011), treeio (Wang et al. 2020), and ggplot2 (Wickham 2016) packages in R software, with the midpoint serving as the root of the tree.

Real-time RT-PCR tests

Specific primers were designed for RT-PCR assays to detect novel viruses in ticks collected from the regions. DNA/RNA was

extracted from adult ticks using the MiniBEST Viral RNA/DNA Extraction Kit (Takara) according to the manufacturer's instructions. RT-PCR reactions were performed using the OneStep RT-PCR Kit (TaKaRa). Initially, 12.5 μl of 2 × 1 Step Buffer, 0.5 μl of forward and reverse primer (10 μM each), 1 μl of PrimeScript OneStep Enzyme Mix, 2 μl of RNA extract, and RNase-free water were added to a 0.2 ml tube to obtain a total volume of 25 μl. The following cycling conditions were used for the RT-PCR: 30 min at 50°C, 3 min at 95°C, followed by 35 cycles of 30 s at 95°C, 30 s at the annealing temperature for each primer pair, 30 s at 72°C, and finally 10 min at 72°C. For the positive samples of the novel viruses, we designed segmented primers based on the complete genome and the RdRp CDS for segmented viruses. We also optimized experimental conditions to amplify the complete RdRp region. RNA was reverse transcribed into cDNA using a PrimeScript IV first-strand cDNA Synthesis Mix Kit (TaKaRa). The cDNA and DNA were amplified using the 2× PCR MasterMix (Thermo Scientific) with the following PCR programmes: 3 min at 95°C, 35 cycles of 30 s at 95°C, 30 s at the annealing temperature of each pair of primer, 30 s at 72°C, and finally 10 min at 72°C. All primers used in this study were provided in Table S1. The amplification products from the positive samples were confirmed by Sanger sequencing.

Results

Sample collection

In 2023, a total of 551 ticks were collected from 14 sampling sites in the desert regions of Xinjiang, China. Morphological identification revealed two tick species from two genera: *Hyalomma asiaticum* and *Rhipicephalus turanicus* (Fig. S1). Among the collected ticks, *H. asiaticum* was the dominant species (65.7%, 362/551), followed by *R. turanicus* (34.3%, 189/551). All *R. turanicus* ticks were collected from livestock, whereas *H. asiaticum* included both questing and blood-feeding ticks. The parasitic ticks were collected from a variety of host animals, including camels, cattle, goats, sheep, and dogs, while the host-seeking ticks were collected from desert and Gobi regions. *H. asiaticum* primarily fed on the buttocks and inguinal areas of livestock, whereas *R. turanicus* attached to the ears of livestock. The adult ticks were pooled into 30 libraries based on collection sites, tick species, sex, and host for meta-transcriptome analysis (Table S2).

Virome diversity of two tick species

A total of 1.82×10^9 150 bp paired-end quality-controlled reads were generated from 30 sequencing libraries in the study. After removing host-related reads, 4 740 331 contigs were *de novo* assembled. Viral reads accounted for 0.004%–0.165% of the total quality-controlled reads within each library, with an interquartile range of 0.03%–0.08%. A total of 1 145 049 RNA viral reads were subsequently classified into 25 families, each of which was highly variable in terms of prevalence and abundance (Fig. 1a). These virus families included 15 families of positive-sense single-stranded RNA (ssRNA(+)) viruses, seven families of negative-sense single-stranded RNA (ssRNA(–)) viruses, three families of double-stranded RNA (dsRNA) viruses. The vertebrate-associated virus family *Phenuiviridae* had high prevalence and abundance in both tick species, while the families *Orthomyxoviridae* and *Nairoviridae* were specific to *R. turanicus*. The family *Chuviridae* showed a relatively high prevalence in *H. asiaticum*, while only one sample of *R. turanicus* was positive. We subsequently obtained a total of 5972 contigs assigned to RNA viruses, from which a total of 125 complete or nearly complete viral genomes were assembled and submitted to GenBank (Table S3). We performed phylogenetic analyses based on the amino acid (aa) of the most conserved RdRp protein (Fig. 2). We classified the viruses according to the demarcation criteria issued by the ICTV (https://talk.ictvonline.org/ictv-reports/ictv_online_report/). A total of 13 families and 28 species of viruses were identified (Table S4), including 14 ssRNA(+) viruses, 10 ssRNA(–) viruses, and 4 dsRNA viruses. Among these 28 viruses, 20 species from 10 families were known viruses, while 8 species from 5 families were novel viruses discovered in this study.

We compared differences in viral composition among samples of two tick species to evaluate the distribution of viruses. The alpha-diversity analysis using Shannon index showed the viral diversity of *R. turanicus* was significantly higher than *H. asiaticum* (Student's *t*-test, *P*-value < .05) (Fig. 1b). However, no statistically significant differences were observed between *H. asiaticum* and *R. turanicus* collected from sheep in the same region, nor between questing *H. asiaticum* and those collected from animals (Fig. S2). We also assessed beta-diversity among samples of two tick species using PCoA, which revealed a significant difference in virome between two tick species. Notably, *H. asiaticum* formed a distinct cluster in the virome compared to samples from *R. turanicus* (Fig. 1c).

Novel vertebrate-associated ssRNA(–) viruses

In this study, three novel vertebrate-associated ssRNA(–) viruses with tick species specificity were identified. A novel segmented virus related to the family *Peribunyaviridae* was discovered in two *H. asiaticum* samples, comprising a large (L) segment and a medium (M) segment, which has been named Desert peribunya-like virus. The RdRp proteins of Desert peribunya-like virus exhibited 81.2% and 81.3% aa similarities to Yushu tick virus 1 (GenBank accession no. ON746492) found in *Dermacentor everestianus* in China (Fig. 3a). The glycoprotein encoded by the M segment exhibited 54.3% and 54.4% aa similarities to Ixodes ricinus bunyavirus-like virus 1 (GenBank accession no. ON684365) found in *Ixodes ricinus* in Croatia (Fig. S3A).

Two novel viruses, Desert orthonairovirus and Desert quaranjavirus, were identified in *R. turanicus*. Desert orthonairovirus belonged to the genus *Orthonairovirus*, and consisted of three segments: L, M, and small (S) (Fig. 3b and c). The L and M segments exhibited the typical terminal reverse complementary sequences characteristic of orthonairoviruses, with a 5′-terminus of UCUCAAAGA and a 3′-terminus of UCUUUGAGA, and were validated by Sanger sequencing. Although the S segment could not be fully assembled at the 5′-terminus, it was assembled to a 3′-terminus of UCUUUGAGA (Fig. 3c and Fig. S3C).

The L segment contained a single open reading frame (ORF) of ~12 kb in length, encoding a protein of 3985-aa, which included a core domain spanning from positions aa 2073 to 2718 (Fig. 3c). The M segment also contained a single ORF encoding a 1436-aa GPC, which was cleaved into two mature membrane glycoproteins, Gn and Gc. Two cleavage sites for the subtilisin-like protease SKI-1/S1P were identified at positions RRLL354↓ and RKLL724↓. The S segment encoded a 483-aa nucleocapsid (N) protein, with an RNA-binding related positively charged region in the C-terminal domain.

Phylogenetic analysis indicated that the three segments of Desert orthonairovirus were closely related to the human pathogenic Wanowrie virus strain Ig700 (Darwsh et al. 1974) and *Orthonairovirus tomdiense* isolate TT1 (Moming et al. 2021), with the RdRp (large protein) showing 79.9% aa similarities (Fig. 3b). The glycoprotein showed 66.4% and 66.5% aa similarities, and the N protein showed 79.9% and 79.1% aa similarities, respectively (Fig. S3B and D). A total of 171 *H. asiaticum* and 86 *R.*

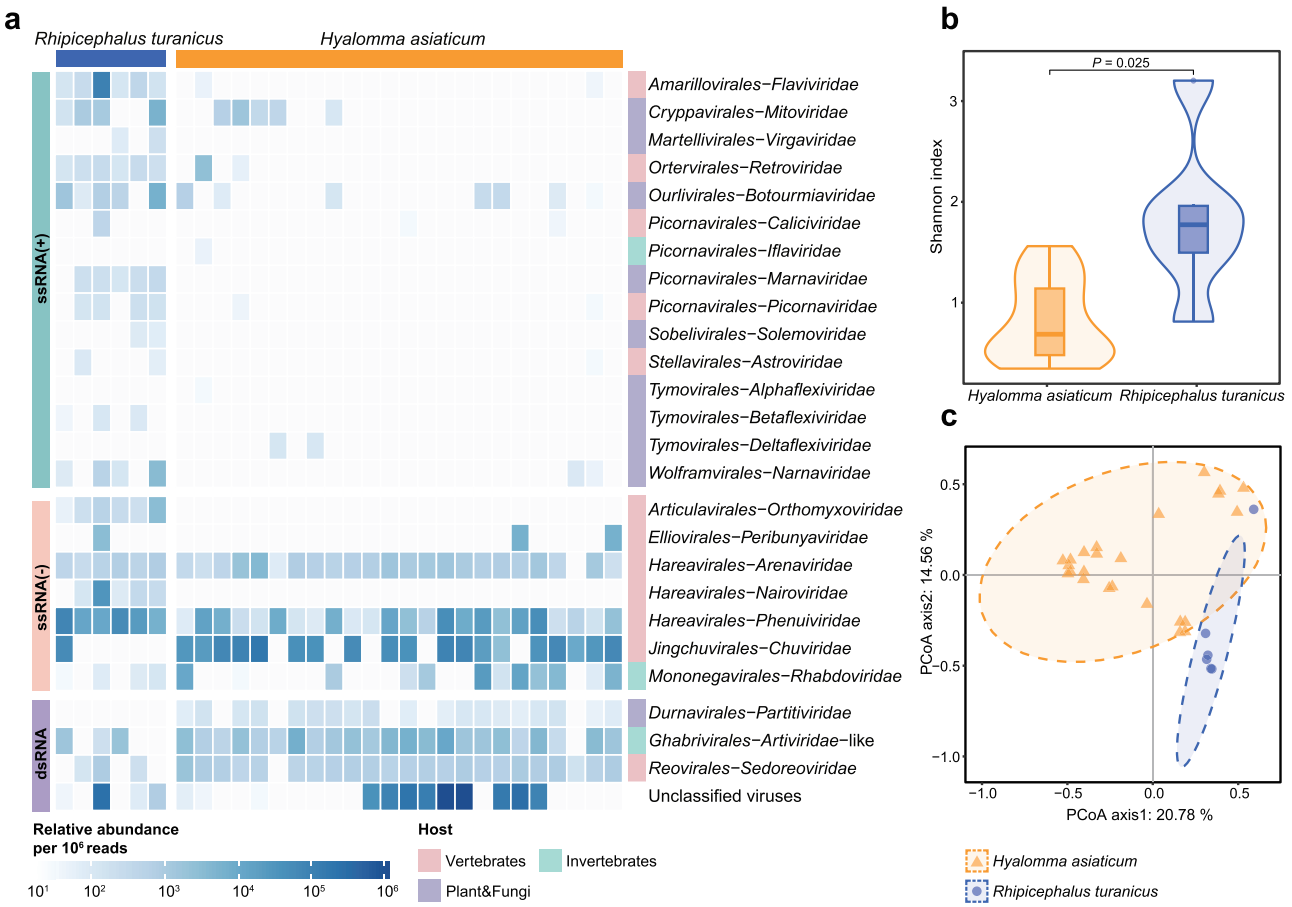

Figure 1. Virus diversity between *H. asiaticum* and *R. turanicus*. (a) Relative abundance profile of viruses between *H. asiaticum* and *R. turanicus*. Each cell in the heat map represents the normalized number of reads belonging to the viral family. (b) Comparison of alpha-diversity of tick viromes (Shannon index) between *H. asiaticum* and *R. turanicus*. Boxplot elements: center line, median; box limits, upper and lower quartiles; whiskers (error bars), the highest and lowest points within 1.5 interquartile range of the upper and lower quartiles. The *P*-value was calculated using a two-sided Student's *t*-test. (c) Between-group clustering of viromes between *H. asiaticum* and *R. turanicus* by PCoA. Presented according to axes 1 (14.56%) and 2 (20.78%).

turanicus samples from the region were tested by RT-PCR using specific primers. One *R. turanicus* sample tested positive for Desert orthonairovirus, and the amplified product sequences were identical to the genomic sequence (Table S5). Previous studies have reported orthonairoviruses primarily in ticks of the genera *Hyalomma, Dermacentor, Ixodes*, and *Haemaphysalis* (Zhang et al. 2018, 2024, 2025, Li et al. 2023), with different tick species serving as vectors for different *Orthonairovirus* viruses. The discovery of this novel Desert orthonairovirus carried by *R. turanicus* broadens the range of vectors for this viral genus.

Desert quaranjavirus, belonging to the genus *Quaranjavirus* in the family *Orthomyxoviridae*, contained six segments, including polymerase basic protein 2 (PB2), polymerase basic protein 1 (PB1), polymerase acid protein (PA), nucleoprotein (NP), hemagglutinin protein (HA), and matrix (M) segments (Fig. 3e). It was identified in five *R. turanicus* samples, and we also screened and amplified two complete PB1 sequences from other *R. turanicus* ticks collected in surrounding areas using specific primers by RT-PCR. Previous studies have indicated that the genus *Quaranjavirus* was associated with large-scale avian mortality events and unexplained fever diseases in children (Taylor et al. 1966, Allison et al. 2015). In this study, the RdRp (PB1) of five Desert quaranjavirus strains exhibited 99.5%–100% aa similarities, showing the highest similarity to Zambezi tick virus 1 (GenBank accession no. MH267793) with 88.2%–88.4% aa similarities (Fig. 3d). However, only the PB1 segment of Zambezi tick virus 1 was available in GenBank. Phylogenetic analysis revealed that Desert quaranjavirus clustered with quaranjaviruses from *Ixodidae* ticks, while other quaranjaviruses from *Argasidae* ticks formed a separate cluster. Further comparison showed that the aa similarities of the Desert quaranjavirus in the PB2, PA, NP, HA, and M segments ranged from 82.3% to 100%, 96.6% to 99.7%, 82.4% to 99.8%, 99.4% to 100%, and 98.1% to 100%, respectively. When compared with Guangdong tick quaranjavirus and *Quaranjavirus* sp. found in *Ixodidae* ticks, the similarities for these segments ranged from 68.7% to 81.3%, 74.0% to 76.6%, 57.7% to 77.5%, 84.9% to 85.9%, and 82.5% to 83.8% (Fig. S3E-I). Compared with Wellfleet Bay virus, Lake Chad virus, and *Quaranjavirus quaranfilense* found in *Argasidae* ticks, the genomic structure of Desert quaranjavirus was consistent with Guangdong tick quaranjavirus detected in *Rhipicephalus* ticks (Fig. 3e). Both lacked the hypothetical viral protein (VP7). Additionally, Granville quaranjavirus found in *Amblyomma dissimile* also lacked the M protein. Compared with other quaranjaviruses, the Desert quaranjavirus genome contained a unique terminal sequence similar to that of Guangdong tick quaranjavirus. Each segment of Desert quaranjavirus contained a highly conserved 5′-terminal sequence, AGCAGAGGCAGC, and a 3′-terminal sequence, CUUGUCUCUACU (Fig. 3f).

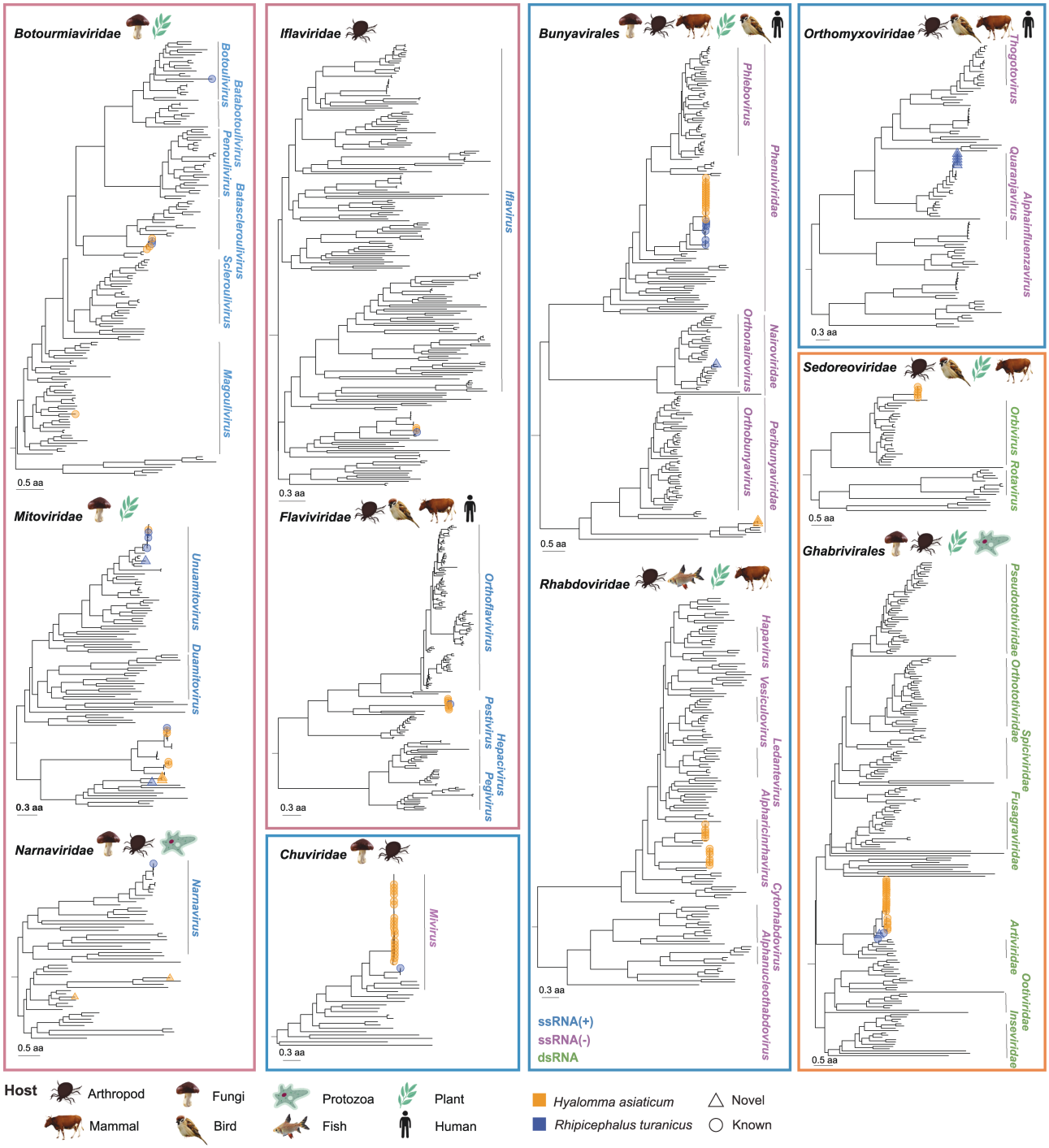

Figure 2. Phylogenetic trees constructed on the RdRp protein for RNA viruses. Newly identified viruses in this study were labelled with triangle; known viruses were labelled with solid circles. Viruses derived from *H. asiaticum* were represented in orange, while those from *R. turanicus* were indicated in blue.

Hyalomma asiaticum-specific viruses

In addition to the potentially pathogenic novel ssRNA(–) viruses, 21 tick species-specific viruses were identified, of which 12 were specific for *H. asiaticum* and nine for *R. turanicus*.

Of the six ssRNA(+) viruses specific to *H. asiaticum*, three were known and three were novel. Bole hyalomma asiaticum virus 1, which was previously detected primarily in *H. asiaticum*, belonged to the family *Iflaviridae* and was detected in three samples of *H. asiaticum* in this study (12.5%, 3/24) (Fig. S4A). Two viruses of the family *Mitoviridae* were detected in *H. asiaticum*, one of which was the novel virus Desert mitovirus 1 (Fig. 4a). *Mitoviridae* sp. was specifically detected in *H. asiaticum* and clustered with sequences previously identified in *R. microplus* from Chongqing, China (Fig. S4B). Two novel *Narnaviridae* viruses specific to *H. asiaticum* were identified (Fig. 4b). The aa similarity of RdRp in Desert narna-like 1 virus to Qingyang Narna tick virus 1 (GenBank accession no. ON746437), found in *Haemaphysalis longicornis* in China, was 58.2%. The RdRp aa similarity of Desert narna-like 2 virus to Aspergillus

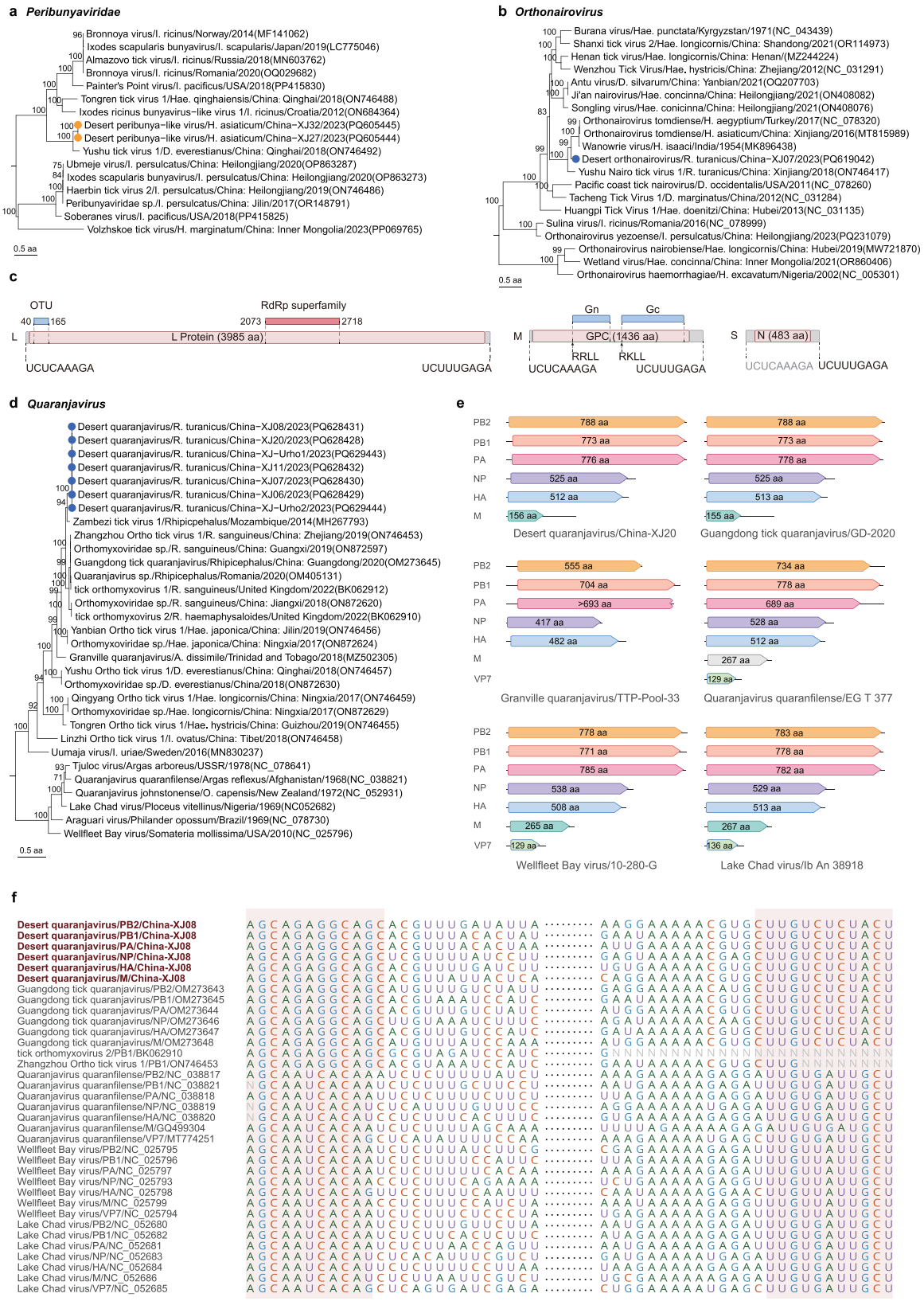

Figure 3. Phylogenetic analysis of vertebrate-associated ssRNA(–) viruses. (a) Phylogeny of viruses in the family *Peribunyaviridae* based on the RdRp protein. (b) Phylogeny of viruses in the genus *Orthonairovirus* based on the RdRp protein. (c) Genomic organization and putative CDSs of Desert orthonairovirus. The large (L) segment encodes L protein, the medium (M) segment encodes glycoprotein precursor (GPC), and the small (S) segment encodes nucleoprotein (N). (d) Phylogeny of viruses in the genus *Quaranjavirus* based on the RdRp protein. (e) Genome structure of Desert quaranjavirus and other quaranjaviruses. PB2, polymerase basic protein 2; PB1, polymerase basic protein 1; PA, polymerase acid protein; NP, nucleoprotein; HA, hemagglutinin protein; M, matrix protein; VP7, viral protein. (f) The terminal sequences of Desert quaranjavirus and other quaranjaviruses. The typical terminal sequences of Desert quaranjavirus and other quaranjaviruses are marked with boxes.

Figure 4. Phylogenetic analysis of *H. asiaticum*-specific viruses. (a) Phylogeny of viruses in the genus *Mitovirus* based on the RdRp protein. (b) Phylogeny of viruses in the family *Narnaviridae* based on the RdRp protein. (c) Phylogeny of *M. boleense* based on the RdRp gene. (d) Phylogeny of Bole Tick Virus 1 based on the RdRp gene. (e) Phylogeny of *A. bole* based on the RdRp gene. (f) Phylogeny of viruses in the order *Ghabrivirales* based on the RdRp protein.

flavus narnavirus 1 (GenBank accession no. LC763254) was 42.6%. Changdu Botou tick virus 1, from the family *Botourmiaviridae*, was detected in only one *H. asiaticum* sample (Fig. S4C).

Among the four *H. asiaticum*-specific ssRNA(–) viruses, *Mivirus boleense* and Bole Tick Virus 1 had higher infection rates of 79.2% and 62.5%, respectively (Fig. 4c and d). Both viruses have primarily been reported in *H. asiaticum*, with *M. boleense* also detected in humans, camels, sheep, and *Rhombomys opimus* in Xinjiang, China. Phylogenetic analysis of Bole Tick Virus 1 revealed two branches, with the strains from this study clustering with the sequences from Xinjiang, China, while the other branch included sequences from other provinces in China. Bole Tick Virus 1 has been reported not only in ticks but also in humans and *Rh. opimus*. In addition, two known viruses in the family *Rhabdoviridae, Alpharicinrhavirus bole* and Taishun Tick Virus, were detected in *H. asiaticum*, which have previously been reported primarily in *Hyalomma* (Fig. 4e and Fig. S4D).

Among the dsRNA viruses specific to *H. asiaticum*, two known viruses were identified (Fig. 4f and Fig. S4E). For the virus from the order *Ghabrivirales*, we constructed a phylogenetic tree of the order using representative viral sequences from 17 families and 19 genera and found that our sequences were genetically most close to the family *Artiviridae*, which were all reported in different kinds of arthropods. According to the latest species classification criteria for this virus order by the ICTV, viruses with more than 70% amino acid identity are considered the same species. Our sequences belong to three distinct virus species. Although they cluster in different branches from previously reported *Totiviridae* sp (Ni et al. 2023), we chose to adopt the terminology of the *Artiviridae* family, and have temporarily named them Desert arti-like virus 1. Desert arti-like virus 1 was found in 24 *H. asiaticum* samples, previously reported in the genus *Hyalomma*. The complete genomes of Yanbian Reovi tick virus 4 in family *Sedoreoviridae* showed 82.8%–83.0% nt similarities to isolate OR1 (GenBank accession no. PP473512) found in *H. asiaticum* in China.

Rhipicephalus turanicus-specific viruses

Among the four ssRNA(+) viruses specific to *R. turanicus*, Desert mitovirus 2 and Desert mitovirus 3, both belonging to the family *Mitoviridae*, were identified (Fig 4a and 5a). The Hulunbuir Botou tick virus 4, a member of the family *Botourmiaviridae*, was detected in one *R. turanicus* sample and clustered with sequences from *D. silvarum* in Heilongjiang, China (GenBank accession no. ON746353) (Fig. 5b). Neofusicoccum parvum narnavirus 2 from the family *Narnaviridae* identified in this study has been previously reported in *D. silvarum* and *Hae. longicornis* in China (Fig. 5c).

Among the three *R. turanicus*-specific ssRNA(–) viruses, Hebei mivirus 1 of the genus *Mivirus* was discovered in one *R. turanicus* sample, which has previously been reported only in *Rhipicephalus* ticks (Fig. 5d). Additionally, Brown dog tick phlebovirus 1 and Tick phlebovirus from the family *Phenuiviridae* were discovered, both of which have primarily been reported in *Rhipicephalus* ticks, with *Tick phlebovirus* showing a high infection rate of 66.7% (Fig. 5e and f).

Among the dsRNA viruses, the *R. turanicus*-specific Desert arti-like virus 2 and Desert arti-like virus 3 were identified (Fig. 4f). The Desert arti-like virus 2 showed 77.4% and 99.7% aa similarity to a *Totiviridae* sp. found in *R. turanicus* from Xinjiang, China (GenBank accession no. ON812617). The Desert arti-like virus 3 showed 73.5% aa similarity to a *Totiviridae* sp. found in *R. haemaphysaloides* from Fujian, China (GenBank accession no. ON81 2598).

Shared ssRNA(+) viruses between two tick species

Among the ssRNA(+) viruses, four were identified as shared between *H. asiaticum* and *R. turanicus*. The *Botourmiaviridae* sp. clustered with sequences from ticks collected in other provinces of China (Fig. 6a). Two *Mitoviridae* viruses, Desert mito-like virus and *Unuamitovirus alar1*, were detected in both *H. asiaticum* and *R. turanicus* (Fig. 6b and c). Bole tick virus 4, belonging to the family *Flaviviridae*, was also detected in both species. Phylogenetic analysis revealed that Bole tick virus 4 formed three distinct clusters according to the tick genera, including *Hyalomma, Rhipicephalus*, and *Dermacentor* (Fig. 6d). The sequences obtained from *H. asiaticum* and *R. turanicus* clustered within the clusters of their same genera. The six sequences from *H. asiaticum* exhibited aa similarities ranging from 98.3% to 99.9%, with *Hyalomma*-derived sequences showing aa similarities between 98.0% and 98.6%. The sequences from *R. turanicus* showed aa similarities ranging from 91.1% to 92.0% with *Rhipicephalus*-derived sequences (Fig. 6e).

Discussion

Desertification is a major challenge in global environmental change. While desertification control efforts have effectively restored some ecosystems worldwide, these processes may also alter vector distribution patterns, thereby increasing the potential for pathogen transmission. In this study, we collected tick samples from desert regions in Xinjiang and performed a metatranscriptomic investigation to analyze the viral diversity of different tick species. A total of 28 tick-borne viruses were identified, with several potentially pathogenic viruses found in *H. asiaticum* and *R. turanicus*, such as the novel Desert peribunya-like virus, Desert orthonairovirus, and Desert quaranjavirus, as well as three known viruses: Bole Tick Virus 1, *M. boleense*, and Bole tick virus 4. In addition, both species-specific and shared viruses were identified in two tick species, highlighting the viral transmission potential and ecological relationships between different tick species, thereby laying the foundation for targeted prevention of potential emerging tick-borne infectious diseases.

Ticks such as *H. asiaticum* and *R. turanicus*, which dominate desert ecosystems in China, are vectors of several zoonotic diseases, posing significant threats to human health and livestock production (Guo et al. 2016, Moming et al. 2018, Liu et al. 2024, Ma et al. 2024). Ticks from desert regions have been found to carry a variety of viruses, including Crimean-Congo hemorrhagic fever virus, Tamdy virus, Tacheng tick virus 1, Tacheng tick virus 2, among them, are pathogenic to humans (Sun et al. 2009, Dong et al. 2019, Liu et al. 2020, Moming et al. 2021). Xinjiang, one of the most desertified regions in China, with its variable climate, unique geography, and active desertification control measures, has created a complex ecological environment that influences vector-host interactions and the transmission dynamics of tick-borne viruses. Our results indicate significant differences in the viral diversity between tick species inhabiting desert environment. We detected high infection rates of known tick species-specific viruses in *H. asiaticum* and *R. turanicus* and identified several novel viruses. Notably, Bole tick virus 4 was detected in both tick species, exhibiting a clear clustering pattern associated with tick genera, suggesting that the viruses carried by different tick genera may have independent evolutionary trajectories. This finding provides a new insight into the viral composition and ecological transmission pathways of ticks in desert regions.

This study identified three novel vertebrate-associated viruses, including Desert peribunya-like virus, Desert orthonairovirus, and

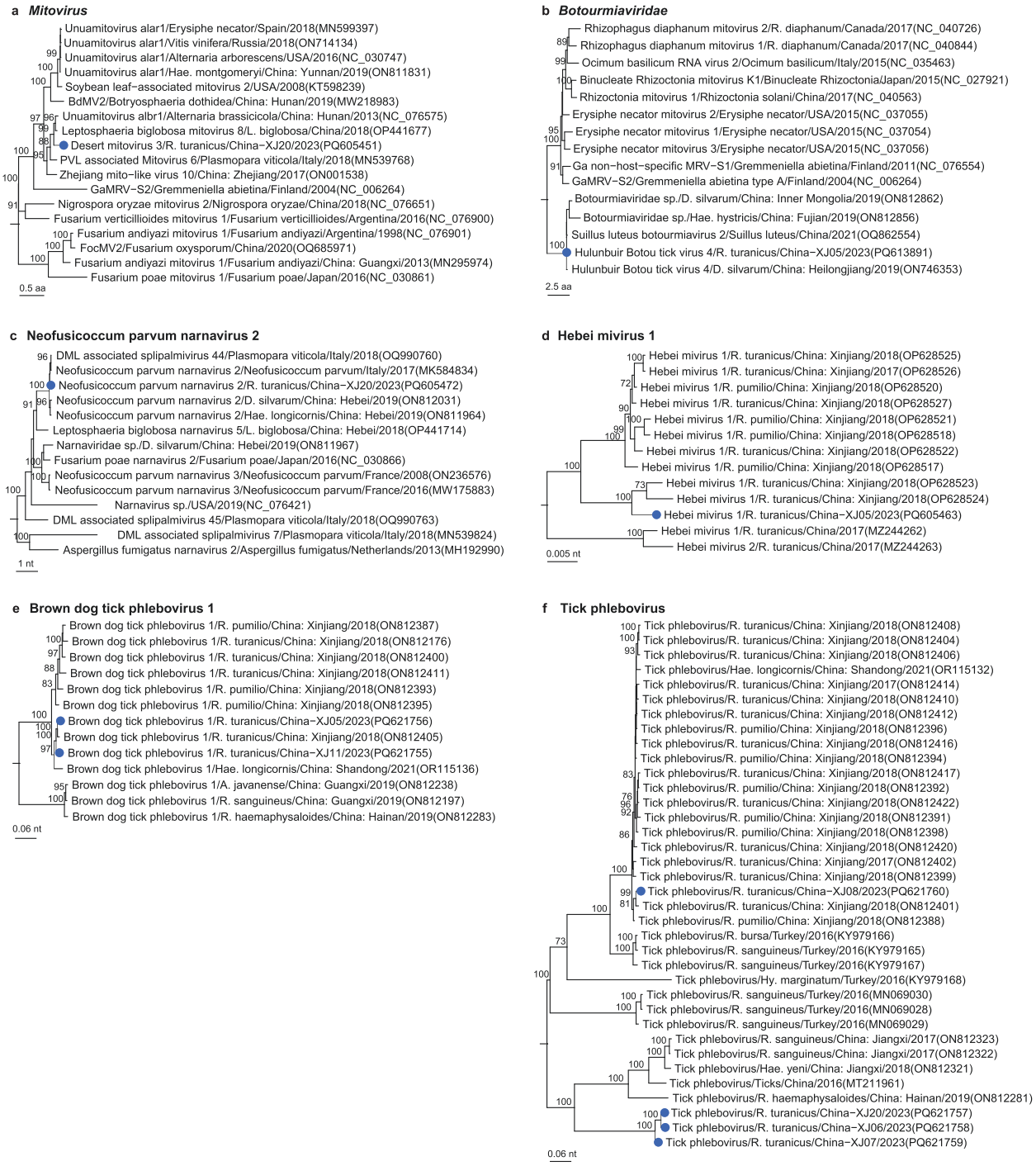

Figure 5. Phylogenetic analysis of *R. turanicus*-specific viruses. (a) Phylogeny of viruses in the genus *Mitovirus* based on the RdRp protein. (b) Phylogeny of viruses in the family *Botourmiaviridae* based on the RdRp protein. (c) Phylogeny of Neofusicoccum parvum narnavirus 2 based on the RdRp gene. (d) Phylogeny of Hebei mivirus 1 based on the RdRp gene. (e) Phylogeny of Brown dog tick phlebovirus 1 based on the RdRp gene. (f) Phylogeny of Tick phlebovirus based on the RdRp gene.

Desert quaranjavirus. Recent discoveries of nairoviruses and their potential to infect humans have attracted increasing attention, particularly with reported cases in Northeast China and Xinjiang (Liu et al. 2020, Ma et al. 2021, Moming et al. 2021, Zhang et al. 2024, 2025). While Crimean-Congo hemorrhagic fever virus has been detected in multiple tick genera, such as *Hyalomma, Rhipicephalus, Argas, Ixodes, Dermacentor*, and *Amblyomma*, other nairoviruses exhibit tick genus specificity (Eslava et al. 2024). For example, Nairobi sheep disease virus was detected only in *Haemaphysalis* and *Hyalomma* (Gong et al. 2013), *O. tomdiense* only in *Hyalomma* and *Dermacentor* (Moming et al. 2024), and Yezo virus only in *Ixodes* (Lv et al. 2023, Zhang et al. 2025). In this study, Desert orthonairovirus was detected in *R. turanicus*, suggesting that this species may serve as its vector. Phylogenetic analysis indicated that the virus is closely related to *O. tomdiense* and Wanowrie virus, which have been found to infect humans, indicating its

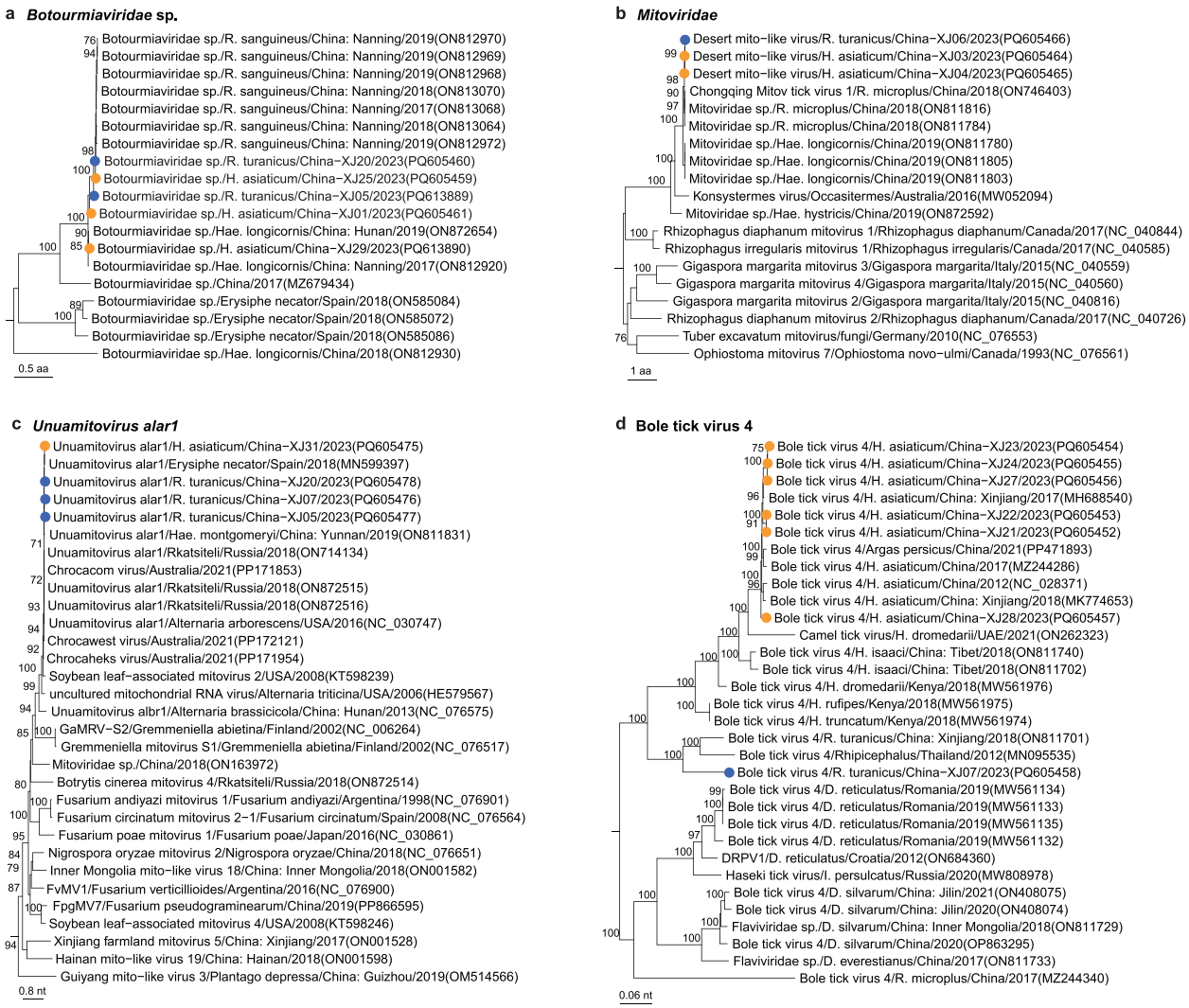

e aa

	MH688540	NC_028371	China-XJ21	China-XJ28	China-XJ24	China-XJ23	China-XJ27	China-XJ22	MN095535	ON811701	China-XJ07	MW561132	MW561134	MW561135
MH688540		98.31	98.45	98.03	98.31	98.27	98.31	98.47	84.99	84.56	84.38	76.26	70.46	82.25
NC_028371	98.31		98.57	98.57	98.36	98.51	98.38	98.59	85.60	85.05	84.78	76.78	70.88	82.75
China-XJ21	98.45	98.57		98.47	98.63	98.59	98.65	99.94	85.48	85.07	84.90	76.74	70.84	82.75
China-XJ28	98.03	98.57	98.47		98.34	98.28	98.36	98.49	85.58	85.09	84.82	76.69	70.76	82.60
China-XJ24	98.31	98.36	98.63	98.34		99.77	99.78	98.65	85.40	84.96	84.82	76.67	70.70	82.63
China-XJ23	98.27	98.51	98.59	98.28	99.77		99.55	98.61	85.40	84.94	84.78	76.65	70.70	82.65
China-XJ27	98.31	98.38	98.65	98.36	99.78	99.55		98.67	85.42	85.02	84.88	76.76	70.78	82.71
China-XJ22	98.47	98.59	99.94	98.49	98.65	98.61	98.67		85.48	85.07	84.92	76.74	70.84	82.75
MN095535	84.99	85.60	85.48	85.58	85.40	85.40	85.42	85.48		93.83	91.05	76.02	70.49	82.33
ON811701	84.56	85.05	85.07	85.09	84.96	84.94	85.02	85.07	93.83		92.03	75.80	70.47	82.06
China-XJ07	84.38	84.78	84.90	84.82	84.82	84.78	84.88	84.92	91.05	92.03		75.82	70.43	82.11
MW561132	76.26	76.78	76.74	76.69	76.67	76.65	76.76	76.74	76.02	75.80	75.82		74.61	86.56
MW561134	70.46	70.88	70.84	70.76	70.70	70.70	70.78	70.84	70.49	70.47	70.43	74.61		82.73
MW561135	82.25	82.75	82.75	82.60	82.63	82.65	82.71	82.75	82.33	82.06	82.11	86.56	82.73	

Figure 6. Phylogenetic analysis of shared ssRNA(+) viruses between two tick species. (a) Phylogeny of *Botourmiaviridae* sp. based on the RdRp protein. (b) Phylogeny of viruses in the family *Mitoviridae* based on the RdRp protein. (c) Phylogeny of *U. alar1* based on the RdRp gene. (d) Phylogeny of Bole tick virus 4 based on the RdRp gene. (e) The comparison between Bole tick virus 4 detected in different tick species. Sequences derived from *H. asiaticum* were marked in an orange box, while that from *R. turanicus* were marked in a blue box.

potential pathogenicity and the need for enhanced surveillance (Darwsh et al. 1974, Moming et al. 2021). These findings not only expand our understanding of tick-borne viruses in desert regions but also highlight the critical role of ticks in cross-species virus transmission.

Desert quaranjavirus, identified in *R. turanicus* in this study, was classified as a member of the genus *Quaranjavirus*, which is characterized by negative-sense single-stranded RNA, with highly conserved and complementary sequences at the ends of each gene segment. Desert quaranjavirus genome was found to consist of six segments, each containing highly conserved and partially complementary terminal sequences, which are critical for the binding of the viral PB1 polymerase subunit and the activation of a unique process called 'cap-snatching' initiated by the PB2 polymerase subunit (Hagen et al. 1995, Presti et al. 2009). Some quaranjaviruses are known to cause unexplained fever in children and avian mortality (Taylor et al. 1966, Allison et al. 2015). Birds, being one of the hosts of *R. turanicus* (Sándor et al. 2021, Toma et al. 2021), likely contribute to viral dissemination. Desert quaranjavirus detected in this study clustered with sequences from distant Mozambique, suggesting a possible link to migratory birds. Xinjiang serves as an important stopover along the East Asia–Australasia, Central Asia–India, and East Africa–West Asia migratory routes. Many migratory birds reside and breed in the wetland oases near Arik Lake and the northern edge of the Gurbantunggut Desert, which surrounds our sampling sites. Desertification control efforts have expanded habitats for migratory birds through environmental restoration, potentially facilitating viral transmission. Previous studies have suggested that climate change and environmental shifts may drive the migration of vectors and their hosts (Carlson et al. 2022). Ecological restoration initiatives are likely to enhance regional vegetation coverage, which could further modulate temperature and humidity dynamics (Ni et al. 2024). The detection of Desert quaranjavirus in ticks parasitizing dogs, goats, and sheep (Table S2), suggests that such environmental improvements may have increased the diversity of animal hosts for ticks, thereby enhancing the habitats overlap between domestic animals and migratory birds and facilitating spillover transmission of pathogens through tick vectors.

A limitation of this study is that tick samples were collected only from specific desert regions in Xinjiang, which may not represent the viral composition of ticks across all desert areas, potentially overlooking viruses with lower infection rates. In addition, *R. turanicus* ticks were not collected at some sampling sites, preventing a comparison of the viral composition between two tick species in the same region and on the same host.

In summary, our study not only revealed the diversity of the tick virome in desert regions, but also provided an in-depth analysis of virus distribution in two tick species, and identified novel tick-borne viruses. These findings provide new insights into virus-vector interactions in desert ecosystems and offer a scientific foundation for assessing the public health risks posed by tick-borne viruses in the desert regions of Xinjiang.

Acknowledgements

Not applicable.

Supplementary data

Supplementary data is available at *VEVOLU Journal* online.

Conflict of interest: The authors declare no competing interests.

Funding

This study was supported by the National Key Research and Development Program of China (2023YFC2305901), the National Science and Technology Fundamental Resource Investigation Program (2022FY100902), and the Postdoctoral Fellowship Program and China Postdoctoral Science Foundation (BX20240215).

Data availability

The sequencing data are available from the NCBI Sequence Read Archive (SRA) (SRR32910946–SRR32910975) under BioProject PRJNA1243690 and the viral genome sequences obtained in this study have been deposited in the NCBI GenBank database (Table S3).

References

Allison AB, Ballard JR, Tesh RB *et al*. Cyclic avian mass mortality in the northeastern United States is associated with a novel orthomyxovirus. *J Virol* 2015;**89**:1389–403.

Bryan BA, Gao L, Ye Y-Q *et al*. China's response to a national land-system sustainability emergency. *Nature* 2018;**559**:193–204.

Buchfink B, Reuter K, Drost H-G. Sensitive protein alignments at tree-of-life scale using DIAMOND. *Nat Methods* 2021;**18**:366–68.

Camacho C, Coulouris G, Avagyan V *et al*. BLAST+: architecture and applications. *BMC Bioinf*. 2009;**10**:421.

Capella-Gutiérrez S, Silla-Martínez JM, Gabaldón T. trimAl: a tool for automated alignment trimming in large-scale phylogenetic analyses. *Bioinformatics* 2009;**25**:1972–73.

Carlson CJ, Albery GF, Merow C *et al*. Climate change increases cross-species viral transmission risk. *Nature* 2022;**607**:555–62.

Chen S-F, Huang T-X, Zhou Y-Q *et al*. AfterQC: automatic filtering, trimming, error removing and quality control for fastq data. *BMC Bioinf*. 2017;**18**:80.

Darwsh MA, Imam ZE, Amer T. Antibodies to Dhori and Wanowrie viruses in Egyptian sera. *J Egypt Public Health Assoc* 1974;**49**:362–68.

Dong Z-H, Yang M-H, Wang Z-D *et al*. Human Tacheng tick virus 2 infection, China, 2019. *Emerg Infect Dis* 2021;**27**:594–98.

Eslava M, Carlos S, Reina G. Crimean-Congo hemorrhagic fever virus: an emerging threat in Europe with a focus on epidemiology in Spain. *Pathogens* 2024;**13**:770.

Gong -S-S, He B, Wang Z-D *et al*. Nairobi sheep disease virus RNA in ixodid ticks, China 2013. *Emerg Infect Dis* 2015;**21**:718–20.

Grabherr MG, Haas BJ, Yassour M *et al*. Full-length transcriptome assembly from RNA-Seq data without a reference genome. *Nat Biotechnol* 2011;**29**:644–52.

Guo L-P, Jiang S-H, Liu D *et al*. Emerging spotted fever group rickettsiae in ticks, northwestern China. *Ticks Tick-borne Dis* 2016;**7**:1146–50.

Hagen M, Tiley L, Chung TD *et al*. The role of template-primer interactions in cleavage and initiation by the influenza virus polymerase. *J Gen Virol* 1995;**76**:603–11.

Jia N, Wang J-F, Shi W-Q *et al*. Large-scale comparative analyses of tick genomes elucidate their genetic diversity and vector capacities. *Cell* 2020;**182**:1328–40.e13.

Langmead B, Salzberg SL. Fast gapped-read alignment with Bowtie 2. *Nat Methods* 2012;**9**:357–59.

Li C-J, Fu B-J, Wang S-A *et al*. Drivers and impacts of changes in China's drylands. *Nat Rev Earth Environ* 2021;**2**:858–73.

Li F, Li J-X, Song J-D *et al*. Novel orthonairovirus isolated from ticks near China–North Korea border. *Emerg Infect Dis* 2023;**29**:1254–57.

Liu G, Tan W-B, Wang H-Q *et al*. The great gerbil (*Rhombomys opimus*) as a host for tick species in Gurbantunggut Desert. *Parasit Vectors* 2024;**17**:55.

Liu X-F, Zhang X, Wang Z-D *et al*. A tentative Tamdy orthonairovirus related to febrile illness in northwestern China. *Clin Infect Dis* 2020;**70**:2155–60.

Lu J, Rincon N, Wood DE *et al*. Metagenome analysis using the Kraken software suite. *Nat Protoc* 2022;**17**:2815–39.

Lv X-L, Liu Z-Y, Li L *et al*. Yezo virus infection in tick-bitten patient and ticks, northeastern China. *Emerg Infect Dis* 2023;**29**:797–800.

Ma J, Lv X-L, Zhang X *et al*. Identification of a new orthonairovirus associated with human febrile illness in China. *Nat Med* 2021;**27**:434–39.

Ma R, Li C-F, Gao A *et al*. Tick species diversity and potential distribution alternation of dominant ticks under different climate scenarios in Xinjiang, China. *PLoS Negl Trop Dis* 2024;**18**:e0012108.

Moming A, Bai Y, Chen S-Y *et al*. Epidemiological surveys revealed the risk of TAMV spill-over from ticks to hosts. *Infect Dis* 2024;**56**:59–65.

Moming A, Shen S, Fang Y *et al*. Evidence of human exposure to Tamdy virus, Northwest China. *Emerg Infect Dis* 2021;**27**:3166–70.

Moming A, Yue X-H, Shen S *et al*. Prevalence and phylogenetic analysis of Crimean-Congo hemorrhagic fever virus in ticks from different ecosystems in Xinjiang, China. *Virologica Sin* 2018;**33**: 67–73.

Nguyen L-T, Schmidt HA, von Haeseler A *et al*. IQ-TREE: a fast and effective stochastic algorithm for estimating maximum-likelihood phylogenies. *Mol Biol Evol* 2015;**32**:268–74.

Ni X-B, Cui X-M, Liu J-Y *et al*. Metavirome of 31 tick species provides a compendium of 1,801 RNA virus genomes. *Nat Microbiol* 2023;**8**:162–73.

Ni X-B, Pei Y, Ye Y-T *et al*. Ecoclimate drivers shape virome diversity in a globally invasive tick species. *ISME J* 2024;**18**:wrae087.

Oksanen J, Simpson G, Blanchet F *et al*. vegan: community ecology package. R package version 2.7-0, 2024. https://github.com/vegandevs/vegan (2 January 2025, date last accessed).

Pal SC, Chatterjee U, Chakrabortty R *et al*. Anthropogenic drivers induced desertification under changing climate: issues, policy interventions, and the way forward. *Prog Disaster Sci* 2023;**20**:100303.

Presti RM, Zhao G, Beatty WL *et al*. Quaranfil, Johnston Atoll, and Lake Chad viruses are novel members of the family *Orthomyxoviridae*. *J Virol* 2009;**83**:11599–606.

Rozewicki J, Li S, Amada KM *et al*. MAFFT-DASH: integrated protein sequence and structural alignment. *Nucleic Acids Res* 2019;**47**:W5–w10.

Sándor AD, Milchev B, Takács N *et al*. Five ixodid tick species including two morphotypes of *Rhipicephalus turanicus* on nestlings of Eurasian eagle owl (*Bubo bubo*) from south-eastern Bulgaria. *Parasit Vectors* 2021;**14**:334.

Schliep KP. phangorn: phylogenetic analysis in R. *Bioinformatics* 2011;**27**:592–93.

Shi M, Lin X-D, Tian J-H *et al*. Redefining the invertebrate RNA virosphere. *Nature* 2016;**540**:539–43.

Sun S-R, Dai X, Aishan M *et al*. Epidemiology and phylogenetic analysis of Crimean-Congo hemorrhagic fever viruses in Xinjiang, China. *J Clin Microbiol* 2009;**47**:2536–43.

Taylor RM, Hurlbut HS, Work TH *et al*. Arboviruses isolated from *Argas* ticks in Egypt: Quaranfil, Chenuda, and Nyamanini. *Am J Trop Med Hyg* 1966;**15**:76–86.

Toma L, Mancuso E, d'Alessio SG *et al*. Tick species from Africa by migratory birds: a 3-year study in Italy. *Exp Appl Acarol* 2021;**83**:147–64.

Wang L-G, Lam TT, Xu S-B *et al*. Treeio: an R package for phylogenetic tree input and output with richly annotated and associated data. *Mol Biol Evol* 2020;**37**:599–603.

Wang Z-D, Wang B, Wei F *et al*. A new segmented virus associated with human febrile illness in China. *New Engl J Med* 2019;**380**: 2116–25.

Wickham H. *Ggplot2: Elegant Graphics for Data Analysis*. New York: Springer, 2016.

Yu G-C, Lam TT, Zhu H-C *et al*. Two methods for mapping and visualizing associated data on phylogeny using ggtree. *Mol Biol Evol* 2018;**35**:3041–43.

Zhang M-Z, Bian C, Ye R-Z *et al*. A series of patients infected with the emerging tick-borne Yezo virus in China: an active surveillance and genomic analysis. *Lancet Infect Dis* 2025;**25**:390–98.

Zhang X-A, Ma Y-D, Zhang Y-F *et al*. A new orthonairovirus associated with human febrile illness. *New Engl J Med* 2024;**391**:821–31.

Zhang Y-F, Shen S, Fang Y-H *et al*. Isolation, characterization, and phylogenetic analysis of two new Crimean-Congo hemorrhagic fever virus strains from the northern region of Xinjiang Province, China. *Virologica Sin* 2018;**33**:74–86.

Zhou H, Xu L, Shi W-F. The human-infection potential of emerging tick-borne viruses is a global public health concern. *Nat Rev Microbiol* 2023;**21**:215–17.

Virus Evolution, 2025, 11(1), veaf022 , DOI: https://doi.org/10.1093/ve/veaf022, Advance Access Publication 19 April 2025, Research Article